

EFFECTS OF THE AGEING TREATMENT ON THE SUPERELASTIC BEHAVIOR OF A NITINOL STENT FOR AN APPLICATION IN THE ESOPHAGEAL DUCT: A FINITE-ELEMENT ANALYSIS

UČINEK STARANJA NA SUPERELASTIČNO VEDENJE NITINOLNE OPORE PRI UPORABI V CEVI POŽIRALNIKA: ANALIZA KONČNIH ELEMENTOV

Fardin Nematzadeh¹, Seyed K. Sadrnezhaad²

¹Materials and Energy Research Center, (MERC), P.O. Box 14155-4777, Tehran, Iran

²Department of Materials Science and Engineering, Sharif University of Technology, P.O. Box 11155-9466, Tehran, Iran
fardinnematzadeh@gmail.com

Prejem rokopisa – received: 2012-10-23; sprejem za objavo – accepted for publication: 2012-12-18

The effects of design parameters and material properties obtained with the ageing treatment on the mechanical performance of a z-shaped esophageal-duct nitinol wire stent under the crushing tests for clinical applications are investigated with a finite-element simulation. With 90 % crushing, low chronic outward force, high radial resistive strength and favorable superelastic behavior are attained at the segment angle of 65° and the A_f temperature of 24 °C. The performance of the stent is seen to drastically vary with a change of only 1° in the segment angle.

Keywords: finite-element analysis, esophageal duct, nitinol stent, ageing treatment, mechanical performance

Z metodo končnih elementov so bili preučevani učinek konstrukcijskih parametrov in mehanske lastnosti materiala pri tlačnih preizkusih starane nitinolne žične opornice z-oblike za klinično uporabo v cevi požiralnika. Z 90-odstotnim tlačenjem, nizko stalno silo navzven, veliko radialno silo upornosti in zeleno superplastično vedenje je bilo doseženo pri segmentu s kotom 65° in temperaturi A_f 24 °C. Opazi se, da se vedenje opore občutno spremeni že pri spremembi kota segmenta za 1°.

Ključne besede: analiza končnih elementov, cev požiralnika, nitinolna opora, staranje, mehansko delovanje

1 INTRODUCTION

Gastrointestinal disease is an important cause of death these days. Renteln et al. have referred to the esophageal cancer as a worldwide source of gastrointestinal malignancies.¹ The majority of patients with esophageal cancer suffers from dysphagia and undergoes death.¹ The primary aim of treating these patients is to reduce dysphagia with a minimum morbidity and mortality and to improve the quality of their lives.¹ With respect to this type of illness, Renteln et al.² have stated that an endoscopic stenting is better than a surgical repair. A stent placement has, therefore, been one of the main remedies for these types of diseases in the last decade.

The use of a stent has two main objectives: (1) a short-term effect of avoiding intimal dissection and an elastic recoil and (2) a long-term effect of avoiding restenosis caused by neointimal hyperplasia mentioned by Stoeckel et al.³ A nitinol-stent placement was developed to introduce a behavioral modality of the palliation of malignant dysphagia. Nitinol stents for the esophageal duct are easily implanted with a low risk of a severe complication. They provide a successful palliation of malignant esophageal obstructions, too. They also help

relieve dysphagia for the patients with inoperable carcinoma esophagus.¹

A stent placement has been the major approach to solving gastrointestinal diseases like esophageal malignancy during the past decade. Nitinol superelastic stents have been considered a solution to the problems such as restenosis after an implantation, a low twisting ability, an unsatisfactory radial mechanical strength and improper dynamic behaviors associated with the ducts.

Owing to a good retrievability and flexibility, the z-shaped wire stents are most widely used in the stent designs.⁴ They can be used to fabricate custom-made stents with preselected values exerting the radial forces for the clinical use. The Z-shaped models are also desirable as, even in a laboratory, they can be easily manufactured by hand. The Z-shaped models also allow various designs with different amounts of radial forces as described by Patrick et al.⁵ Important parameters like the length, diameter of the wire, number of bends, segment angle, stent inner diameter and radial contraction should be determined with analytical equations associated with the geometry of a stent.

The first report about a numerical study of the fatigue behavior of a nitinol stent was presented by Whitcher et al.⁶ A good agreement of their numerical results, calcu-

lated for the crushing tests, with the other researchers' experimental data was assessed by Petrini et al.⁷, Kleinstreuer et al.⁸ have offered a computational analysis of different nitinol stent-graft combinations for the support of the abdominal aortic aneurysm (AAA). Beule et al.⁹ have developed the strategies to investigate and optimize the mechanics of braided stents. Silber et al.¹⁰ have shown the effect of changing geometrical characteristics on the mechanical properties of the nitinol wire stents. The finite-element method is useful for designing the knitted nitinol meshes utilized in a prospective external vein reinforcement.¹¹

Liu et al.¹² have performed critical testing for determining the pseudoelastic behavior and transformation temperatures of the near-equiatomic NiTi shape-memory alloys. Duerig et al.⁴ have compared the mechanical performance of self-expanding stents usable for the treatment of a vascular disease. It has been shown that the NiTi A_f temperature has a great influence on the mechanical performance of self-expandable stents. Yeung et al.¹³ have shown that the A_f temperature of a nitinol alloy can be controlled by manipulating the heat-treatment parameters. This is important for the production of the nitinol stents with favorable superelastic behavior. Patel et al.¹⁴ have studied the effect of the active A_f temperatures on the fatigue properties of nitinol. They have shown that a low A_f temperature has a short fatigue-life consequence. Liu et al.¹⁵ have evaluated the effect of age treatment on the shape-setting and superelasticity of the Ti-50.7 % Ni stents. They have shown that the optimum ageing temperature for the production of the expected shape of a stent is 500 °C with an ageing time of no more than 60 min resulting in an excellent non-linear superelasticity with the maximum recoverability at the body temperature. To achieve the superelastic behavior of a stent, A_f should be lower than the body temperature. Its optimum value depends on the stiffness needed for a removal of a duct obstruction. A low A_f causes problems like high stiffness and augmented radial forces that can lead to an injury and scars on the duct.

Although there is some information available on the nitinol wire stents, to the best of our knowledge, the z-shaped wire stents for esophageal ducts have not been

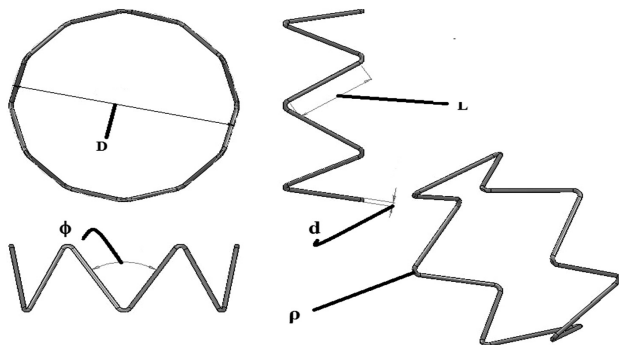


Figure 1: Geometric parameters of a Z-shaped esophageal stent
Slika 1: Geometrijski parametri Z-oblike opornice za cev požiralnika

studied before. The purpose of this investigation is, hence, an application of the finite-element method for an elucidation of the effects of the design parameters and material properties obtained from the ageing treatment on the mechanical performance of the nitinol stents designed for esophageal ducts. The effects of important parameters are predicted via the model calculations and are verified with the experimental information available in the literature. The model is developed on the basis of the nonlinear 3D finite-element method. An application of the results can help diminish dysphagia, improving the quality of patients' life.

2 MODELING AND METHODS

2.1 Geometric models

Micro-CT can be used for obtaining the optimum geometry of the commercial stents available on the market. This instrument is, however, not useful for designing innovative new designs. The geometry of the stent used in this research was, therefore, generated by a computer-aided three-dimensional interactive application (Catia v.5 (Dassault Systèmes, USA)) and transformed into a finite-element-analysis code. The geometric parameters of the esophageal stent are sketched in **Figure 1** and quantified in **Table 1**. The geometric parameters shown in **Figure 1** and **Table 1** were based on the age treatment of the Ti-50.7 % Ni alloy at 500 °C for respective durations of 60 min and 30 min according to the clinical reports given in the literature.^{1,15}

Table 1: Geometric values for the stents of this research (unit of length is mm)

Tabela 1: Geometrijske vrednosti za opore v tej raziskavi (enota dolžine je mm)

Sample	Internal diameter of stent (D)	Radius of curvature (ρ)	Segment length (L)	Diameter of wire (d)	Bending angle (ϕ)
Sample 1	25.0	0.3	10.03	0.2	66°
Sample 2	25.0	0.3	10.80	0.2	65°

2.2 Material properties

The properties of the nitinol stents considered for esophageal ducts are evaluated with a crushing test. Superelastic wire properties are merely considered in an evaluation of the clinical behavior of the nitinol stents used in this research. The model first developed by Auricchio et al.¹⁶ and Lubliner et al.¹⁷ and then significantly extended by Rebelo et al.¹⁸ is used for the simulation of the nitinol superelastic behavior. The model is based on a generalization of the theory of plasticity and the second law of thermodynamics written in terms of Helmholtz free energy. In this theory, the strain is decomposed into two components:

$$\Delta \epsilon = \Delta \epsilon^{el} + \Delta \epsilon^{tr} \quad (1)$$

in which $\Delta\epsilon^{el}$ is the elastic strain and $\Delta\epsilon^{tr}$ is the transformation strain. The transformation of austenite to twinned martensite occurs due to the motion of the shear forces taking place in the stress-threshold range of the superelastic material according to the following equations:

$$F^S \leq F \leq F^F \tag{2}$$

in which F is the transformation potential and S and F denote the martensite transformation start and finish, respectively;

$$\Delta\epsilon^{tr} = a\Delta\zeta \frac{\partial F}{\partial \sigma} \tag{3}$$

$$\Delta\zeta = f(\sigma, \zeta)\Delta F \tag{4}$$

$$F = \bar{\sigma} - p \tan \beta + CT \tag{5}$$

in which a is the coefficient of strain, ζ is the martensite percentage, σ is the von Mises stress, $\bar{\sigma}$ is the von Mises equivalent stress, p is the pressure, β and C are the material constants and T is the temperature. A similar approach is applied to define the reverse transformation which takes into account different stress

thresholds. Equations 3 and 4 define the transformation intensity. Any change in the stress direction generates a martensite reorientation with a negligible additional attempt. Furthermore, the model includes a linear shifting of the stress thresholds with the temperature. In view of the fact that there is a volume increase associated with the transformation, less stress is needed to generate a transformation in tension and, specifically, in compression. This effect is modeled with the linear Drucker-Prager approach for the transformation potential shown in equation 5 and referred to by Rebelo et al.¹⁸ The parameters required in the Abaqus 6.10 (Dassault Systèmes, Providence, RI, USA) user-material subroutine for the nitinol material based on the Auricchio model for opening the esophageal duct are summarized in **Table 2**.^{12,15,19} The basis for the material-property selection of the stents is the age treatment results of the Ti-50.7 % Ni alloy at 500 °C for 30 min and 60 min. The data given for the sample No. 1 from **Table 2** is based on the age treatment of the Ti-50.7 % Ni alloy at 500 °C for 30 min. The data for the sample No. 2 from **Table 2** is based on the age treatment of the Ti-50.7 % Ni alloy at 500 °C for 60 min. A typical nitinol superelastic behavior employed in this research is illustrated in **Figure 2**. Before testing, a cubic element of nitinol is considered and its results are compared with the experimental data. Based on the comparative experimental and mathematical curves plotted in **Figure 3**, it is recognized that the Auricchio model is in reasonable agreement with the empirical data and, consequently, hereafter, the properties of the materials are defined in a subroutine based on the aforementioned numerical model.

Table 2: Material properties used in the simulation of an esophageal-duct opening with a nitinol stent. The data are based on the Auricchio model.^{12,15,19}

Tabela 2: Lastnosti materiala, uporabljene v simulaciji odpiranja nitinolne opore požiralnika. Podatki temeljijo na Auricchiovem modelu.^{12,15,19}

Symbol	Description	Sample No. 1	Sample No. 2
E_A	Austenite elasticity	24100 MPa	20700 MPa
ν_A	Austenite Poisson's ratio	0.33	0.33
E_M	Martensite elasticity	17800 MPa	11700 MPa
ν_M	Martensite Poisson's ratio	0.33	0.33
ϵ^L	Transformation strain	0.054	0.055
$\left(\frac{\partial \sigma}{\partial T}\right)_L$	stress/temperature ratio during loading	5.32 MPa T ⁻¹	5.32 MPa T ⁻¹
σ_L^S	Start of transformation loading	390 MPa	344 MPa
σ_L^E	End of transformation loading	401 MPa	363 MPa
T_0	Reference temperature	37 °C	37 °C
$\left(\frac{\partial \sigma}{\partial T}\right)_U$	Stress/temperature ratio during unloading	5.32 MPa T ⁻¹	5.32 MPa T ⁻¹
σ_U^S	Start of transformation unloading	112 MPa	58 MPa
σ_U^E	End of transformation unloading	93 MPa	42 MPa
σ_{CL}^S	Start of transformation stress in compression	-	-
ϵ_V^L	Volumetric transformation strain	0.054	0.055
A_f	Austenite finish transformation temperature	22 °C	24 °C
ϕ	Segment bending angle	66°	65°

2.3 Meshing and boundary conditions

Hypermesh (Altair® Hypermesh® v. 6.0) is a high-performance finite-element preprocessor that provides highly interactive software for the performance analysis of a product design. It is noticeable that due to the meshing problems caused by a small section of the nitinol wire and a relatively complex geometry of the stents, the hypermesh software is used to mesh the samples. The

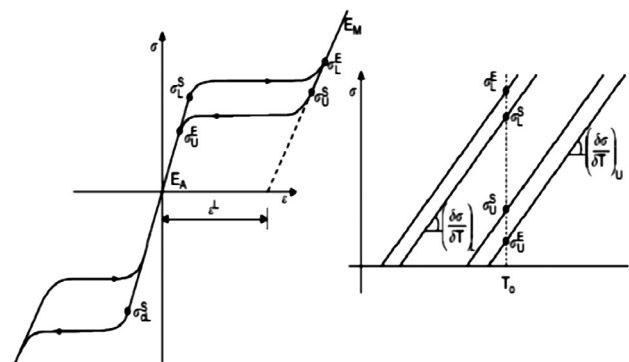


Figure 2: Typical behavior of superelastic nitinol
Slika 2: Značilno vedenje superelastičnega nitinola

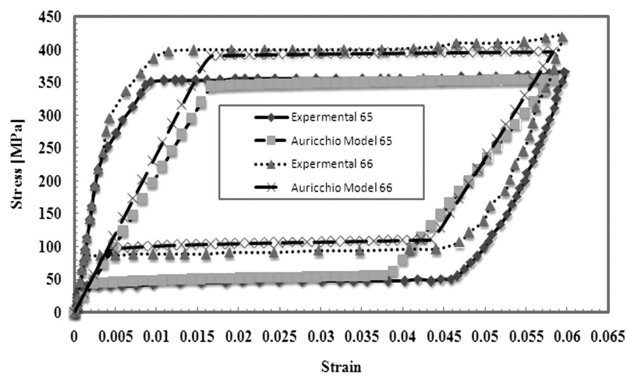


Figure 3: Comparison of the Auricchio-model calculations with the experimental data obtained for the superelastic nitinol samples No. 1 (66°) and 2 (65°) from **Table 2**

Slika 3: Primerjava izračunov po Auricchiovem modelu z eksperimentalnimi podatki za superplastične vzorce nitinola št. 1 (66°) in št. 2 (65°) iz **tabele 2**

mesh parameters for the esophageal stent during crushing are listed in **Table 3**. Using the Abaqus contact module, only the contact between the outer stent surface and the inner plane surfaces is activated. In this contact algorithm, the master surface for the rigid planes and the slave surface for the stent are concurrently applied. A penalty interaction property is employed to enforce the impermeable boundaries. Two inflexible similar plates are applied for the pressure on the stent. The distance between the two planes is 25 mm (equal to the stent nominal diameter value in the expanded configuration). The rigid-flexible contact pairs are formed between the planes and the surfaces of the stent and no friction is considered for any contact pair. According to Petrini et al.,⁷ the lower plane is fixed in all directions and the higher plane can just move in the Y direction. Four stent nodes close to the planes are fixed in the X and Z directions. As a result, the stent can be compressed just in the Y direction. Displacement loading is thus applied on the higher plane: the higher plane compresses the stent and reduces the distance between the two planes to 7.5 mm (a 70 % reduction in the diameters of the stents) and 2.5

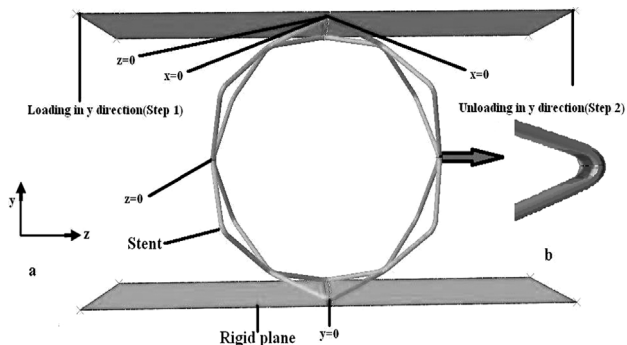


Figure 4: a) Schematic representation of the boundary conditions for the crushing of the esophageal stent, b) exact position of the stent, for which numerical calculations have been performed

Slika 4: a) Shematski prikaz robnih pogojev za tlačenje opore požiralnika, b) točen položaj opore, kjer so bili izvršeni numerični izračuni

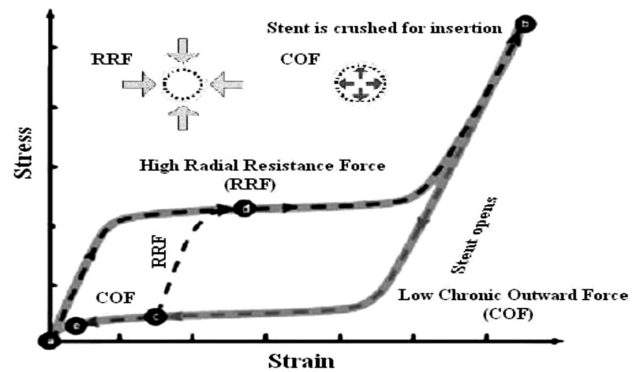


Figure 5: RRF and COF of a typical superelastic hysteresis loop¹⁵
Slika 5: RRF in COF značilne superelastične histerezne zanke¹⁵

mm (a 90 % reduction in the diameters of the stents). The higher plane then moves back to its first location and recovers the stent. The reaction force on the plane is collected during the compression and recovers the process. The boundary conditions for the crushing of the esophageal-duct stent are shown in **Figure 4**. To decrease the calculation time and use the benefits of the axis symmetry, only one-quarter of the geometrical model is analyzed. The temperature is adjusted to 37 °C (the body temperature) during the simulation.

3 RESULTS AND DISCUSSION

Duerig et al.⁴ have shown a favorable clinical performance of the nitinol stents used for esophageal application due to a complete superelastic hysteresis loop, the lowest chronic outward force (COF), the highest radial resistive force (RRF) and the long plateau stress. Gideon et al.²⁰ have shown that a lower stress and a higher strain on the critical points of a stent allow a suitable clinical performance. COF and RRF are related to the superelastic behavior of a nitinol stent. A typical superelastic stress-strain curve for a self-expanding stent is shown in **Figure 5**.¹⁵ The stent is crushed by two rigid planes (path a-b) and later deployed, reaching stress equilibrium with the duct at point c. The force against the duct is controlled with the unloading curve (COF) and the force resisting deformation is controlled with the loading curve (RRF). Generally, stent designers aim for as high an RRF as possible, with as low a COF as possible.⁴ Furthermore, two particular points should be considered so that the stents are never in the elastic region. In addition, the stents are known for having a satisfactory superelastic behavior. Moreover, the stents should be in the failure-safe domain from mechanical strength and strain.²¹ Beule et al.⁹ have shown that an increase in the segment angles, radial contraction of the stent and decrease in the length of the segments improve the performance of the stent. Their study indicates, however, that due to the transformation-temperature (A_T) effects, in the case of a lower angle and longer segments, a better superelastic performance is gained with the nitinol stent.

Table 3: Mesh parameters for the esophageal stent during crushing
Tabela 3: Parametri mreže za oporo požiralnika med stiskanjem

Material	Element type	Number of elements	Number of nodes
Stent	C3D8I	3600	14400
Rigid plane	R3D4	20000	20402

Table 4: Results for stress, strain and displacement of the esophageal stent under 70 % crushing

Tabela 4: Rezultati napetosti, raztezka in radialnega raztezka opore požiralnika pri 70-odstotnem stiskanju

Stent model	Maximum stress (MPa)	Maximum strain	Radial displacement
Sample 1 from Table 2	269.9	0.00862	0.00642
Sample 2 from Table 2	229.9	0.00850	0.011

Table 5: Results for stress, strain and displacement of the esophageal stent under 90 % crushing

Tabela 5: Rezultati napetosti, raztezka in radialnega raztezka opore požiralnika pri 90-odstotnem stiskanju

Stent model	Maximum stress (MPa)	Maximum strain	Radial displacement
Sample 1 from Table 2	486.8	0.0152	0.00246
Sample 2 from Table 2	373.5	0.0146	0.00340

This advantage is consistent with the observations of Beule et al.⁹ Every nitinol stent with a high A_f temperature (close to the body temperature) will be in the lower COF range with a better fatigue life. A nitinol stent of an acceptable performance does not require a high RRF for a low obstruction of esophageal ducts. With a high obstruction of esophageal ducts, the A_f temperature of nitinol should be much lower than the body temperature due to the need for a high RRF.

With respect to the nitinol stents illustrated in **Figure 1** and quantified in **Table 1**, this paper first discusses the results of the 70 % standard crushing according to Petrini et al.⁷ and then the results of the 90 % crushing. According to **Table 4**, the maximum stress, strain and displacement during the 70 % crushing show an elastic behavior of the esophageal stents. A comparison of sample No. 1 from **Table 2** and sample No. 2 from **Table 2** indicates that a decrease in the maximum stress from 269.9 MPa to 229.9 MPa results in an insignificant reduction in the maximum strain from 0.00862 to 0.00850. The maximum radial displacement increases from 0.00642 to 0.011 under the same conditions. This increasing ratio is about 71.3 %. Also, these stents, owing to the non-superelastic behavior, are not suitable for esophageal applications. According to the stent shown in **Figure 1** and **Table 1** (sample No. 1 from **Table 2**), the minimum stress to initiate a martensitic transformation is 390 MPa. The stress level of this stent is not sufficient for achieving the superelastic behavior.

Consequently, this stent is not appropriate for an esophageal application. Therefore, discussing other test results of the stent has no meaning. As a result, the desired superelastic behavior is not achieved. Finally, considering the non-superelastic behavior, the stent would not be suitable for an esophageal-stent application. With the material properties of sample No. 2 from **Table 2**, the minimum stress to initiate a martensite transformation is 344 MPa. Discussing the test results for the stents with unacceptable stress levels is not necessary, even if they can provide a normal spring behavior. As a result, the desired superelastic behavior is not achieved with the stents that have very low stresses. According to **Table 5**, a comparison of sample No. 1 from **Table 2** and sample No. 2 from **Table 2** indicates that a decrease in the maximum stress from 486.8 MPa to 373.5 MPa results in a insignificant reduction in the maximum strain from 0.0152 to 0.0146. The maximum radial displacement increases from 0.00246 to 0.00340 under the same conditions. This increasing ratio is about 38.2 %. The maximum stress on the internal curvature of the stent of sample No. 2 from **Table 2** is lower than that of sample No. 1 from **Table 2**. The former is, hence, preferred to the latter. The maximum strain on the internal curvature of the stent of sample No. 1 from **Table 2** is slightly higher than that of sample No. 2 from **Table 2**. Consequently, the former helps the dynamic motion of the stent to be in harmony with the duct. In summary, despite the fact that the standard crushing level is 70 %, the stents showed no superelastic behavior at this crushing level. An increase in the crushing from 70 % to 90 % results in an appearance of the superelastic behavior and produces a favorable condition for fabricating esophageal stents. This indicates that the designed stents are capable of withstanding higher strain forces of up to 90 % while preserving the superelastic behavior. In addition, a failure of a stent with this value is safe.²¹ With 90 % crushing, the stent shown in **Figure 1** and quantified in **Table 1** (sample No. 2 from **Table 2**) exhibits a more acceptable mechanical performance as far as the material properties are concerned. Considering the properties of the materials used in **Table 2** (samples 1 and 2) at 22 °C and 24 °C, respectively, there should be a different range of loading and unloading plateau stress. A lower A_f temperature of nitinol and extensive loading and unloading stress levels of the mechanical hysteresis are related to the superelastic behavior. Duerig et al.⁴ have shown that a difference of 7 °C in the A_f temperature results in about a 50 % variation in the stress level. Patel et al.¹⁴ have shown that a decreasing A_f temperature results in a higher upper plateau stress. **Figure 6** shows an increase in the upper plateau stress due to the difference between the A_f temperatures of 22 °C and 24 °C. For a difference of 2 °C, the expected 15 % variation has been confirmed with the experimental and numerical results⁴. The angular difference between the stent geometries illustrated in **Figure 1** and **Table 1** is

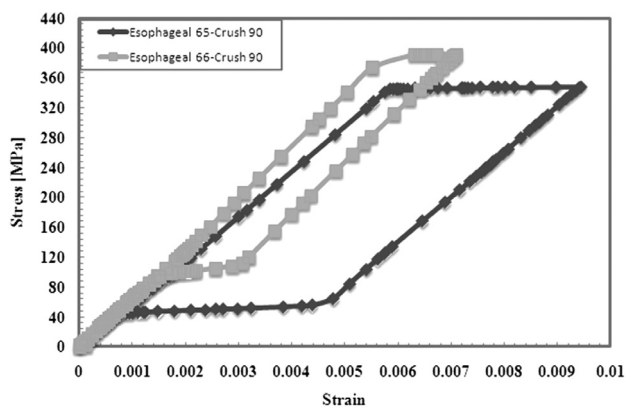


Figure 6: Comparison of the superelastic behavior of the 90 % crushed esophageal-duct stent with the material properties of sample No. 1 (66°) and 2 (65°) from **Table 2**

Slika 6: Primerjava superelastičnega vedenja 90-odstotno stisnjene opornice požiralne cevi z lastnostmi materiala vzorca št. 1 (66°) in št. 2 (65°) iz **tabele 2**

only 1 degree. The basis for the aforementioned geometric design results from the age treatment of the Ti-50.7 % Ni alloy at 500 °C and the time intervals of 30 min and 60 min.¹⁵ However, the stent shown in **Figure 1** and **Table 1** (sample No. 2 from **Table 2**) reveals a more acceptable mechanical and practical performance in comparison with that illustrated in **Figure 1** and **Table 1** (sample No. 1 from **Table 2**). Nevertheless, according to **Figure 1** and **Table 1** (sample No. 1 from **Table 2**) and considering the short segments of the stent and a wider angle between the stent segments, better geometric conditions for the crushing test are achieved and a more reasonable mechanical performance is expected as described by Beule et al.⁹ The acceptable mechanical performance of the stent from **Figure 1** and **Table 1** (sample No. 2 from **Table 2**) is mainly rooted in its material properties obtained by the ageing treatment of the Ti-50.7 % Ni alloy at 500 °C, the time interval of 60 min and the optimum angle of 65°.¹⁵ The results of the numerical calculations performed for the curve of the stent in **Figure 4b** obtained with crushing under a high pressure are demonstrated in **Figure 6**. Consequently, based on the desired mechanical standards of the stents and according to **Figure 6**, the stent shown in **Figure 1** and quantified in **Table 1** (sample No. 2 from **Table 2**) with a low COF, high RRF, superelastic behavior related to the hysteresis loop and no stress concentration at the internal curvature of the stent is preferred to the other types.

4 LIMITATIONS

This simulation is complex because of the contacts, non-linear geometry, the material nonlinearity, large deformation, additional buckling and bending of the stent. On the other hand, during crushing, the self-contact phenomenon (the contact between the edges of the

stent) is anticipated and it can cause additional stress at the contact points. However, according to Wu et al.,²² owing to the superelasticity behavior of the stent, these types of stress can be neglected. The crushing tests have only been performed in the longitudinal orientations. It is obvious that more experiments and simulation results related to the stenosis degree of ducts are needed to reach to a comprehensive conclusion.

5 CONCLUSIONS

The effects of design parameters and material properties obtained from the ageing treatment on the mechanical performance of the z-shaped nitinol stents for esophageal ducts are investigated. A nitinol stent shows a better mechanical and practical performance owing to only a 1-degree angular difference between the segments of the stent. The material is the Ti-50.7 % Ni alloy, age treated at 500 °C for a 30 min to 60 min time interval. The nitinol stent with the segment angle of 65°, crushing of 90 % and the A_f temperature of 24 °C having a low COF and high RRF shows a favorable superelastic behavior and a low stress concentration on the internal curvature. The superelasticity and hysteresis behavior of nitinol are proven to be promising properties for the z-shaped wire stents used for fabricating esophageal ducts.

Acknowledgments

The authors would like to thank Dr. Amir R. Khoei, professor at Civil Engineering Department, Sharif University of Technology and Mr. Ehsan Haghghat, research assistant at McMaster University for assisting with the implementation of the simulation program to model the samples. We would also like to thank Mr. Seyed M. Seyed Salehi, PhD student at Material Science and Engineering Department, Sharif University of Technology for many helpful discussions on the numerical analysis of the stents.

6 REFERENCES

- ¹ K. Hameed, H. Khan, R. Din, J. Khan, A. Rehman, M. Rashid, Self-Expandable metal stents in palliation of malignant esophageal obstruction, *Gomal J. Med. Sci.*, 8 (2010), 39–43
- ² D. Renteln, B. Walz, B. Riecken, T. Kayser, K. Caca, Endoscopic management of acute esophageal dissection by using a covered self-expanding metal stent, *Gastro. Endoscopy*, 69 (2009), 577–580
- ³ D. Stoeckel, A. R. Pelton, T. Duerig, Self-expanding Nitinol stents: material and design considerations, *Eur. Radio*, 14 (2004), 292–301
- ⁴ T. Duerig, D. Tolomeo, M. Wholey, An overview of superelastic stent Design, *Min. Invas. Ther. and Allied Technol.*, 9 (2000), 235–246
- ⁵ B. Patrick, B. Snowhill, L. John, L. Randall, H. Frederick, Characterization of Radial Forces in Z Stents, *Inves. Radiology*, 36 (2001), 521–530
- ⁶ F. D. Whitcher, Simulation of in vivo loading conditions of Nitinol vascular stent structures, *Comput. Struct.*, 64 (1997), 1005–1011

- ⁷ L. Petrini, F. Migliavacca, P. Massarotti, S. Schievano, G. Dubini, F. Auricchio, Computational studies of shape memory alloy behavior in biomedical applications, *J. Biomech. Eng.*, 127 (2005), 716–725
- ⁸ C. Kleinstreuer, Z. Li, C. Basciano, S. Seelecke, M. Farber, Computational mechanics of Nitinol stent grafts, *J. Biomech.*, 41 (2008), 2370–2378
- ⁹ M. Beule, S. Cauter, P. Mortier, D. Loo, R. Impec, P. Verdonck, B. Verheghe, Virtual optimization of self-expandable braided wire stents, *Med. Eng. Phys.*, 31 (2009), 448–453
- ¹⁰ G. Silber, M. Alizadeh, A. Aghajani, Finite element analysis for the design of Self-expandable Nitinol stent in an artery, *I. J. Energ. Tech.*, 2 (2010), 1–7
- ¹¹ H. V. D. Merwe, B. D. Reddy, P. Zilla, D. Bezuidenhout, T. A. Franz, Computational study of knitted Nitinol meshes for their prospective use as external vein reinforcement, *J. Biomech.*, 41 (2008), 1302–1309
- ¹² Y. Liu, S. P. Galvin, Criteria for pseudoelasticity in near-equiatomic NiTi shape memory alloys, *Acta Materialia*, 45 (1997) 11, 4431–4439
- ¹³ K. Yeung, K. Cheung, W. Lu, C. Chung, Optimization of thermal treatment parameters to alter austenitic phase transition temperature of NiTi alloy for medical implant, *Mater. Sci. Eng. A*, 383 (2004), 213–218
- ¹⁴ M. Patel, D. Plumley, R. Bouthot, The Effects of Varying Active A_f temperatures on the Fatigue Properties of Nitinol Wire, *Proc. of ASM Conf.*, Boston, 2005, 1–8
- ¹⁵ X. Liu, Y. Wang, D. Yang, M. Qi, The effect of ageing treatment on shape-setting and superelasticity of a Nitinol stent, *Mater. Charact.*, 59 (2008), 402–406
- ¹⁶ F. Auricchio, R. Taylor, Shape-memory alloys: Modeling and numerical simulations of the finite-strain superelastic behavior, *Comput. Methods Appl. Mech. Engrg.*, 143 (1997), 175–194
- ¹⁷ J. Lubliner, F. Auricchio, Generalized plasticity and shape memory alloy, *I. J. Solid. Struct.*, 33 (1996), 991–1003
- ¹⁸ N. Rebelo, N. Walker, H. Foadian, Simulation of implantable stents, *Abaqus user's conf.*, 143 (2001), 421–434
- ¹⁹ A. G. Prince, G. L. Quarini, J. E. Morgan, J. Finlay, Thermomechanical response of 50.7 % Ni-Ti alloy in the pseudoelastic regime, *Mater. Sci. Tech.*, 19 (2003), 561–565
- ²⁰ V. Gideon, P. Kumar, L. Mathew, Finite Element Analysis of the Mechanical Performance of Aortic Valve Stent Designs, *Trends Biomater. Artif. Organs*, 23 (2009), 16–20
- ²¹ A. R. Pelton, V. Schroeder, M. Mitchell, X. Gong, M. Barneya, S. Robertson, Fatigue and durability of Nitinol stents, *J. Mech. Behav. Biomed. Mater.*, 1 (2008), 153–164
- ²² W. Wu, M. Qi, X. Liu, D. Yang, W. Wang, Delivery and release of Nitinol stent in carotid artery and their interactions: a finite element analysis, *J. Biomech.*, 40 (2007), 3034–3040